

The construction of a nose shape of minimum drag for specified external dimensions and volume using Euler equations[☆]

N.L. Yefremov, A.I. Kraiko, K.S. P'yankov, S.A. Takovitskii

Moscow, Russia

Received 30 May 2006

Abstract

The problem of constructing the axisymmetric nose shape which gives minimum wave drag for a specified volume and external dimensions is solved by a direct method using Euler equations. As in the Newton's formula approximation, the optimum contours together with the front faces – a segment of the boundary extremum along the longitudinal coordinate and the gently sloping segment of the bilateral extremum – may contain a cylindrical end part with a horizontal segment of the boundary extremum with respect to the maximum admissible radial coordinate. In the direct method, the required parameters (“controls”), which define the shape of the optimum contour, are the radii corresponding to the points of the segment of a bilateral extremum, including the radius of the face for fixed abscissas. For each aspect ratio (the ratio of the length to the radius of the base), when a certain value of the volume coefficient (the ratio of the volume to the volume of a cylinder of maximum external dimensions) is exceeded, the optimum nose shape is completed by a rear cylindrical part. The optimum nose shape, which begins from a certain initial contour, that satisfies the limitations of the problem, is constructed after a finite number of cycles. In each cycle, all the controls are corrected, and together with the directions of the change, their increments are found, while the information necessary for this for any number of controls is obtained after three direct calculations. One other advantage of the method is the rapid, close to quadratic, convergence. The nose shapes constructed are compared with the nose shapes that are optimum in the Newton's formula approximation.

© 2007 Elsevier Ltd. All rights reserved.

1. Introduction

Many pure and applied mathematicians have been interested in problems of constructing a nose shape of minimum wave drag, beginning with Newton,^{1,2} in different formulations. The problem of the optimum axisymmetrical nose shape of specified aspect ratio (“Newton's problem”), solved by Newton using an approximate formula, which he proposed (“Newton's formula”) for determining the pressure on the surface of a body in a gas flow, was the first problem of the variational calculus. The most important element of its solution – the front face – is a segment of a boundary extremum, which occurs due to constraints on the maximum admissible length, while in the Newton's formula approximation it is simultaneously due to the presence of limits on its applicability.^{3–5} When solving problems of optimum design using Newton's formula, the second is as important as the first. If, as shown in Fig. 1a, the x axis of cylindrical coordinates x, r is directed along the free-stream velocity vector V_∞ , while the equation of the required contour is written in the form $x = X(r)$ with $X(0) = 0$ and $X(R) = L$, where L and R are the length and radius of the base of the forebody then in

[☆] *Prikl. Mat. Mekh.* Vol. 70, No. 6, pp. 1017–1030, 2006.

E-mail address: akraiko@ciam.ru (N.L. Yefremov).

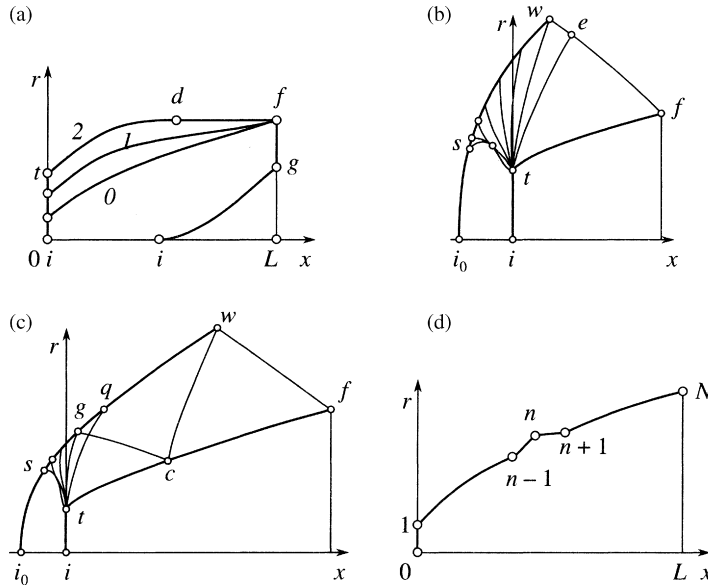


Fig. 1.

Newton’s problem these constraints take the form

$$0 \leq X(r) \leq L, \quad 0 \leq \vartheta \leq \frac{\pi}{2}, \quad \text{ctg } \vartheta = X' \equiv \frac{dX}{dr} \tag{1.1}$$

In view of these constraints on the face, only unilateral variations are admitted: $\delta X \geq 0, \delta \vartheta \leq 0$. For this reason, there is no need here to satisfy the necessary conditions of optimality, which represent the main content of classical courses in the variational calculus (when using Newton’s formula on the face when the necessary condition for an extremum is satisfied in the form of Euler equation, Legendre’s condition – the necessary condition for a minimum – breaks down). Recently, however, despite the widely held opinion (see Ref. 6, p. 78) it has been pointed out that “Newton’s problem obtains a natural and standard solution only within the modern theory of optimal control, but such a natural and standard solution of this problem has not been obtained within the framework of the variational calculus”.

The above assertion is untrue for two reasons. First, a consideration of segments of the boundary extremum is as natural and simple as determining the maximum and minimum of a function of one variable in a finite interval, and, in addition to the extrema (points of zero derivative – analogues of the classical extremals of the variational calculus) one need only calculate its value at the ends of the interval. Second, in Refs 1–5, the solution of Newton’s problem is obtained precisely within the framework of the variational calculus without using such instruments of the modern theory of optimal control as Pontryagin’s and Bellman’s maximum principle, and linear and dynamic programming. Finally, in the classical course on the variational calculus (Ref. 7, p. 238–243) the face in Newton’s problem is regarded as a segment on which only unilateral variations of X are admitted, and it is emphasised that $X(r)$ is a non-decreasing function. The latter is equivalent to the constraints on ϑ according to (1.1).

Another occasion on which Newton only made a few brief assertions on this problem without proof, consisted of a single “lecture” (Ref. 2, p. 428–430), mainly occupied with comments by Krylov). The “lecture” touched upon three themes: (1) the construction of a drag-optimum truncated cone of specified length and base radius (eleven lines and a figure), (2) the reduction in the drag of a solid of revolution when the oval part adjoining the nose is replaced by intersecting segments of tangents with angles of inclination to the axis of rotation of 90° and 135° (one sentence and a figure), and (3) the shape of a gently sloping part of optimum contour, adjoining the front face (ten lines and a figure). The law, defining the shape of this part, was written in the form of the ratio of the lengths of the four rectilinear segments connected with it. The methods of obtaining this ratio, presented in Refs 1,2, in the comments of 18-th Century translators, are also far from resembling the familiar apparatus of the variational calculus. A corresponding derivation using this apparatus is given by Krylov in Ref. 2. However, neither Newton nor Krylov in the comments gave reasons for the occurrence of a front face, and it is precisely this fact which was particularly important for aerodynamicists who

were concerned, in the middle of the 20-th Century, with solving Newton's problem. In fact, if we take into account constraints (1.1), the basis for introducing a face could be Newton's "first and second" assertions. From these, as Krylov showed,² there follows the necessary condition for a minimum: $X' \geq 1$, which is stronger than Legendre's condition $X' \geq 1/\sqrt{3}$.

Newton's problem was solved in Ref. 8 using Euler equations, which described the axisymmetric flow of a perfect (non-viscous and non-heat-conducting) gas. As previously,^{1–5} the contours constructed include a front face – a segment of a boundary extremum, the reason for the occurrence of which is now related solely to the constraint on the length of the nose shape, and with the smooth gently sloping part with a corner point adjoining it. For low-aspect ratios $l = L/R$ the gently sloping part is obtained as the exact solution of a variational problem. For aspect ratios exceeding a certain amount, depending on the free-stream Mach number M_∞ , a similar exact solution requires the introduction initially of one and then (as the aspect ratio increases) a larger number of internal corner points, of which even one with the strongest kink slightly affects the drag value. For high l contours were constructed in Ref. 8, which do not satisfy one of the optimality conditions which defines the main kink. In this sense they are said to be "close to optimum". The fact that the front face is a segment of a boundary extremum was shown in Ref. 8 by comparing the drag of bodies obtained by different admissible variations of the front face.

Until recently the nose shape of minimum drag, with constraints different from the external-dimension constraints, were only constructed in the Newton's formula approximation. Attempts in Refs 9,10 to construct the optimum nose shape for a specified base radius R and a specified volume Ω were unsuccessful, since the authors of these papers, not understanding the reasons why the front face occurs in Newton's problem, attempted to construct a solution with a front face and a free length, as in Newton's problem. In these solutions, for dimensionless volumes, $0 \leq \omega \equiv \Omega/(\pi R^3) \leq 313\sqrt{3}/3645 \approx 0.149$ the optimum nose shape with a front face with $0.346 \approx \sqrt{3}/5 \leq \omega \leq \infty$ is a pointed nose shape and when $0.149 \leq \omega \leq 0.346$ it was confirmed that the "solution, if one exists, cannot be obtained in the formulation considered".¹⁰ The solution of this problem in the same formulation was constructed in Ref. 11 (see also Ref. 5) for all ω : pointed nose shapes are optimum over a smaller range ($0.433 \approx 13/30 \leq \omega \leq \infty$), a basically new configuration is optimum, namely, a spike ig , protruding from the rear face gf (Fig. 1a). The rear face, like the front face in Newton's problem, is a segment of the boundary extremum, by virtue of the previous constraints (1.1) with the difference that now, of the constraints on X , the second one rather than the first is essential.

In the Newton's formula approximation, for slender bodies the problem of the optimum nose shape for specified external dimensions and volume, more accurately, l and ω or the volume coefficient $C_\Omega = \Omega/(\pi R^2 L)$, was considered in Ref. 12. The solution turned out to be incomplete, since the equations and conditions obtained there¹² only enable one to construct optimum nose shapes when $0.25 \leq C_\Omega \leq 0.5$, i.e. only in a quarter of the total range of values of the volume coefficient ($0 \leq C_\Omega \leq 1$). A complete solution of this problem was obtained in Ref. 13 using Newton's formula. The contours of the optimum nose shapes, constructed without the assumption that the forebodies are slender, together with the segment of a bilateral extremum and front and/or rear faces may contain a cylindrical section – one more segment of the boundary extremum, which occurs due to constraint the maximum admissible radius.

If p is the pressure, ρ is the density and $V = |\mathbf{V}|$, as previously, the subscript ∞ indicates free-stream parameters, r_f is the radius of the front face and $r = r(x)$ is the equation of the gently sloping part of the contour, the drag coefficient is given by

$$C_x = \frac{1}{\rho_\infty V_\infty^2 R^2} \int_0^R (p - p_\infty) dr^2 = \frac{2}{\rho_\infty V_\infty^2 R^2} \left[\int_0^{r_f} (p - p_\infty) r dr + \int_0^L (p - p_\infty) r r' dx \right] \quad (1.2)$$

Graphs of C_x of the optimum nose shapes as a function of $0 \leq C_\Omega \leq 1$ for different l , obtained in Ref. 13, are shown in Fig. 2, in a more simplified form than in Ref. 13. The end points of the curves $C_x = C_x(C_\Omega, l)$ correspond to the minimum and maximum possible volumes ($C_\Omega = 0$ and 1). For these, according to Newton's formula, $C_x = 1$. For each l the circles show the value of C_x of the nose shape of Newton's problem, which is a minimum for this l . Between the circles and the triangles the optimum contours have a front face and a gently sloping segment of a bilateral extremum. The triangles correspond to the limitingly thick forebodies of this kind with a horizontal tangent at the point f . At the right of these the contours consisting of the front face, a gently sloping part and a rear cylinder $r \equiv R$ are optimum.

In direct methods, the required contour is specified by N parameters, which play the role of controls. As the controls we can take the radii corresponding to $N - 1$ points on the gently sloping part of the contour for fixed x and the abscissa of the initial point of the cylindrical part. The gently sloping part can be approximated by splines or other functions.

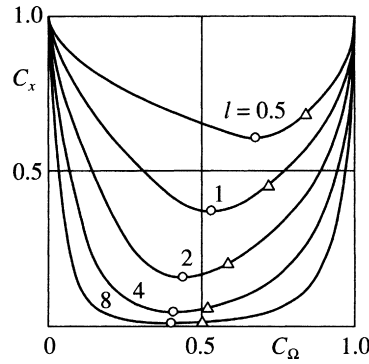


Fig. 2.

In this case, the number of controls (the parameters of these functions) will be less. Irrespective of the choice of the controls, classical direct methods possess two drawbacks. First, in order to use them, each correction requires a number of the direct calculations of the flow around the optimized configuration, which equals the number of controls. Second, the use of only the first derivatives (the gradient) in multidimensional control space yields very poor (linear) convergence to the optimum. As a result, these methods are extremely costly as regards the required computer resources and computing times.

By combining the direct method with the “general method of Lagrange multipliers”, we can, in principle, obtain the information required for the next correction of the optimized contour, after one direct calculation. Using the general method of Lagrange multipliers^{4,8} with arbitrary isoperimetric constraints, in particular, with fixed volume Ω or fixed volume coefficient C_Ω , the increment of the drag coefficient ΔC_x for admissible variations of the “short” forebody (Fig. 1b, the thin curves are the C^+ - and C^- -characteristics, and the sonic line is ts) is given by the formula

$$\Delta C_x = A\Delta r_t + B\Delta x_t + \left(\int_i^{t^-} + \int_{t^+}^f \right) D\delta x dr \tag{1.3}$$

Here $\Delta r_t, \Delta x_t \geq 0$ and δx are the increments of the coordinates of the point t and the variation of x on the segments of the boundary (it^-) and bilateral (t^+f) extrema, while the coefficients A, B and D are known functions of r , the flow parameters and the Lagrange multipliers μ_1, μ_2 and μ_3 on the contour itf .

For the forebody of the type considered, constructed in the previous iteration, the flow parameters are found from the solution of the direct problem, while the Lagrange multipliers are found from the conjugate problem. The equations of the conjugate problem, linear in μ_i , have the same characteristics as the flow equations, and are solved in the “reverse” direction – from the C^- -characteristic wf , where μ_i are known. The complete solution of the conjugate problem is extremely complex. However, to determine μ_i and, together with them, the coefficient D on the segment t^+f one must solve the conjugate problem solely in the triangle tef for known values of μ_i on the segment ef and a single condition on the segment t^+f for a supersonic flow. Then, the isoperimetric constraints only manifest themselves in the condition on t^+f . Compared with direct calculations of the flow around a blunt forebody with a detached shock wave i_0w , the numerical solution of the conjugate problem in the triangle tef presents no difficulties.

A knowledge of the coefficients B at the point t and D on the face it^- is necessary to prove that the face is a segment of the boundary extremum, rather than for constructing the optimum contour. In contrast to this, the values of D on the part t^+f , obtained after solving the conjugate problem in the triangle tef , in practice, as a result of one direct calculation of the flow around the nose shape, determine the direction of the required changes in x over the whole gently sloping segment, apart from the point t . Unlike D on t^+f , the coefficient A can only be obtained after solving all the conjugate problems, and this, as already pointed out, is extremely difficult. Hence, to determine the direction of the change in r_t one more direct calculation is required with a slightly changed r_t .

A similar situation also occurs for “long” nose shape (Fig. 1c) with the sole difference that now the conjugate problem must be solved in the tetragon $tqwf$. This is not much more complicated than for a short nose shape (Fig. 1b). It is true that now the characteristics cw, cg and gt in general will be lines of discontinuity of the multipliers μ_i , as a result of which, in formula (1.3) for ΔC_x there will now be additional terms outside the integrals, related to increments of the

coordinates of the point c . When constructing close to optimum nose shapes with a smooth part tf , these terms can be neglected. However, in principle, the admittance of a corner point and the resulting slight complication of the conjugate problem enable us, using this approach, to construct a configuration with an internal corner point. Thus, apart from the dependence on the number of parameters, which specify the nose shape with a front face, the inclusion of the general method of Lagrange multipliers reduces to two the number of direct calculations required for the next correction. At the same time, a second drawback is the linear convergence to an optimum when this approach is retained.

Since the Sixties and Seventies of the last century, approaches based on “sensitivity analysis” have become widely used (see the review Ref. 14), and not only in relation to optimization problems. In direct methods for constructing optimum aerodynamic shapes, these approaches became used somewhat later. However, at the present time there is a considerable literature on the use of sensitivity analysis for optimal design in aerodynamics. A fairly complete representation of its possibilities when constructing configurations, in the perfect gas flows can be found in Refs 15–21. Like the Lagrange multipliers and the factor D expressed in terms of them in formula (1.3), the sensitivity coefficients, which are key for direct methods with a sensitivity analysis, are found in the process of a single direct calculation of the flow. Another fact, relating these approaches, is that one of the methods of determining the sensitivity coefficients consists of solving the conjugate problem which, in its strict realization, is equivalent to the conjugate problem of the Lagrange multipliers method. Finally, judging by the required number of iterations in Ref. 20, up to recently direct methods with a sensitivity analysis, like the approach with the Lagrange multipliers method, had linear convergence. More rapid (quadratic) convergence is possible using sensitivity coefficients of the first and second orders (the second functional derivatives with respect to the controls). A method of determining them simultaneously was developed in Ref. 21.

In recent years, direct methods, based on “genetic algorithms” have become extremely popular.^{22–24} However, even in comparatively simple problems their realization requires parallel calculations on microprocessor systems. Here, despite the reduction in the number of controls, due to the use of Bézier splines or other approximating functions and the simplicity of paralleling, the use of genetic algorithms is justified primarily in multicriterial problems (for Pareto optimization).

2. Formulation of the problem and a direct method of constructing optimum nose

The values of C_x calculated in Ref. 13 by integration of the equations of the perfect flow for the nose shapes, constructed there using Newton’s formula, confirmed the advantages of convex configurations. In contrast to this, C_x of nose shapes with concave parts and all the more with base faces, as a rule, exceeded C_x of the equivalent cones. At the sometime, in the examples, where the advantage of such nose shapes preserved, it was considerably less than that obtained using Newton’s formula. One of the consequences of these results is a change in the formulation of the variational problem. In practice, the specification of the volume of the forebody is due to the arrangement in it of a useful load of fixed volume Ω_f . For this volume the nose shape must satisfy the inequality $\Omega \geq \Omega_f$. If Ω^0 corresponds to the solution of Newton’s problem with a free volume $\Omega^0 \geq \Omega_f$, then precisely this with $C_x = C_x^0$, which is a minimum for specified l , gives a solution of the problem. According to Fig. 2, in this case a considerable reduction in the drag is possible (when $l \geq 1$, several fold). From a mathematical point of view, such a nose shape can be regarded as a hollow fairing with walls of zero thickness with the useful volume Ω_f inside. Consequently, nose shapes that are optimum when using Newton’s formula with $C_\Omega = C_\Omega^0$, corresponding to the parts of the curves to the left of the small circles in Fig. 2, including *igf* in Fig. 1a, are of no interest.

Taking the above into account, henceforth the coordinates of the contours of the optimum forebodies and their volume coefficients will satisfy the constraints

$$0 \leq x \leq L, \quad 0 \leq r \leq R, \quad C_\Omega^0 \leq C_\Omega = \frac{1}{LR^2} \int_0^L r^2 dx \leq 1 \quad (2.1)$$

The coefficients C_Ω^0 and C_x^0 for specified l , M_∞ and the specific heat ratio κ correspond to the solution of Newton’s problem using Euler equations, which describe the perfect flow, gas.

As already noted, in the approximation of these equations, gently sloping segments (segments of a bilateral extremum) of the optimum contours in Newton’s problem can contain internal corner points, although their pres-

ence has practically no effect on the drag value. Gently sloping segments, which in the problem solved later, are constructed by the direct method, are obtained smooth. The need to introduce internal corner points into them (in the accurate formulation) is easily established by the variation, proposed in Ref. 25, in the characteristic “ε-strips” (see also Refs 4,5,8). Using it, it can be shown that only nose shapes with non-zero slope of the tangent ϑ_{f-} at end points (type 0 and 1 in Fig. 1a) can have internal corner points. However, for such nose shapes with a reduction in ϑ_f , the value and effect of the corner point are also reduced, while for contours with $\vartheta_{f-} = 0$, and all the more with a cylindrical rear section, a gently sloping part is smooth. Neglect of such corner points in the problem considered is even more justified than in Newton’s problem.

The direct method used henceforth was employed previously in Refs 26–32 to construct optimum nose shapes with no constraints on the volume, symmetrical airfoils, solitary wings and wings under conditions of aerodynamic interference with other components of the aircraft. In view of the features of the method which merit attention and the sketchiness with which they are described in Refs 26–32, we will give a more complete description of it.

The basis of the method is the representation of the increment of the drag by a quadratic form. When constructing it, local linearization is employed, which gives a relation between the increments of the pressure and the change in the orientation of small elements of the contour or surface in the flow. The conditions for a minimum of the quadratic form lead to equations that ensure a close-to-quadratic rate of convergence to the optimum. Already after the first correction, aerodynamic shapes are obtained which are close to optimum in the drag value. This method enables one to obtain an analytic solution for a number of problems within the framework of Euler equations. Thus, for Newton’s problem truncated nose shapes are obtained having a power generatrix with an exponent of 2/3.³¹ For $M_\infty = 2$ and $M_\infty = 4$ their C_x exceed C_x of the optimum nose shapes by no more than 3% and 1% respectively. As the aspect ratio increases the diameter of the front face approaches zero, while the power contour with exponent 2/3, as in the case of Newton’s formula, is independent of M_∞ . The exponent obtained as $l \rightarrow \infty$ within the framework of Newton’s formula is 3/4.

We will begin the description of the method employed with the example of a nose shape without a cylindrical part. We will take as the controls the values r_n of the radii of the ends of the $N - 1$ segments of the gently sloping part of the nose shape with fixed x_n ($n = 1, \dots, N$). Of the coordinates of the front face r_1 and $x_1 = 0$ and of the base $r_N = R$ and $x_N = L$, only r_1 is the control. The mean parameters on the segments will be assigned semi-integer subscripts, for example (Fig. 1d) $h_{n-1/2} = x_n - x_{n-1}$. In accordance with this, the formulae for χ - the integral of the pressure forces, acting on the forebody, and its volume $\Omega \geq \Omega^0$, apart from positive factors which will be unimportant later, take the form

$$\begin{aligned} \chi &= \int_0^{r_1} p r dr + \int_0^L p r r' dx = \int_0^{r_1} (p - p_\infty) r dr + p_\infty \frac{r_1^2}{2} + \int_0^L p r r' dx = \frac{K r_1^2}{2} + \int_0^L p r r' dx \approx \\ &\approx \frac{K r_1^2}{2} + \sum_{n=1}^{N-1} (p r r' h)_{n+1/2}, \quad \Omega = \int_0^L r^2 dx \approx \frac{1}{3} \sum_{n=1}^{N-1} (r_n^2 + r_n r_{n+1} + r_{n+1}^2) h_{n+1/2} \end{aligned} \tag{2.2}$$

$$K = \rho_\infty V_\infty^2 \left(c_{x0} + \frac{1}{\kappa M_\infty^2} \right), \quad c_{x0} = c_{x0}(M_\infty, \kappa) = \frac{1}{r_1^2} \int_0^{r_1} \frac{p - p_\infty}{\rho_\infty V_\infty^2} dr^2$$

Here $r_1 = r_t$ is the radius of the front face while c_{x0} is its wave drag coefficient. For comparatively slight kinks at the point t the quantity c_{x0} is independent of the shape of the gently sloping part t^+f . This condition is satisfied everywhere henceforth.

A change in the radii r_n yields changes in the angles of inclination of the segments ϑ and the pressure p acting on them. Following the assumptions introduced earlier^{26–32} we will assume that the relation between the increments Δp and $\Delta \vartheta$ is the same as for local linearization of the flow equations with respect to the parameters of the initial supersonic flow (but differing from the free stream) on the same segments. In this approximation, it is reduced to the formula for a simple wave (μ is the M angle)

$$\Delta p \approx \rho V^2 \text{tg} \mu \Delta \vartheta \approx A \Delta \text{tg} \vartheta, \quad A = \rho V^2 \text{tg} \mu \cos^2 \vartheta$$

In accordance with this

$$\begin{aligned} \operatorname{tg} \vartheta_{n-1/2} &= \frac{r_n - r_{n-1}}{h_{n-1/2}}, \quad \Delta(\operatorname{tg} \vartheta_{n-1/2}) = \frac{\Delta r_n - \Delta r_{n-1}}{h_{n-1/2}} \\ \Delta p_{n-1/2} &\approx A_{n-1/2} \frac{\Delta r_n - \Delta r_{n-1}}{h_{n-1/2}}, \quad \Delta p_{n+1/2} \approx A_{n+1/2} \frac{\Delta r_{n+1} - \Delta r_n}{h_{n+1/2}} \end{aligned} \tag{2.3}$$

According to relations (2.2) and (2.3), the increments $\Delta\chi$ and $\Delta\Omega$, apart from squares of Δr_n , are given by the expressions

$$\begin{aligned} \Delta\chi &= \left[Kr_1 - \left(Arr' + rp - pr' \frac{h}{2} \right)_{3/2} \right] \Delta r_1 + \left[\frac{K}{2} - \left(\frac{Ar' + p}{2} - \frac{A}{h} r \right)_{3/2} \right] (\Delta r_1)^2 - \\ &- 2 \left(\frac{A}{h} r \right)_{3/2} \Delta r_1 \Delta r_2 + \sum_{n=2}^{N-1} \left\{ \left[\left(Arr' + rp + pr' \frac{h}{2} \right)_{n-1/2} - \left(Arr' + rp - pr' \frac{h}{2} \right)_{n+1/2} \right] \Delta r_n + \right. \\ &\left. + \left[\left(\frac{Ar' + p}{2} + \frac{A}{h} r \right)_{n-1/2} - \left(\frac{Ar' + p}{2} - \frac{A}{h} r \right)_{n+1/2} \right] (\Delta r_n)^2 - 2 \left(\frac{A}{h} r \right)_{n+1/2} \Delta r_n \Delta r_{n+1} \right\} \end{aligned} \tag{2.4}$$

$$\begin{aligned} 3\Delta\Omega &= (2r_1 + r_2)h_{3/2}\Delta r_1 + h_{3/2}(\Delta r_1)^2 + h_{3/2}\Delta r_1\Delta r_2 + \sum_{n=2}^{N-1} \{ [(r_{n-1} + 2r_n)h_{n-1/2} + \\ &+ (2r_n + r)h_{n+1/2}]\Delta r_n + (h_{n-1/2} + h_{n+1/2})(\Delta r_n)^2 + h_{n+1/2}\Delta r_n\Delta r_{n+1} \}, \quad \Delta r_N = 0 \end{aligned}$$

To obtain the necessary conditions for a minimum of χ for fixed Ω , setting up the Lagrange functional $I = \chi + 3\lambda\Omega$ with undetermined constant multiplier λ , we equate the derivatives of ΔI with respect to Δr_n to zero with $n = 1, 2, \dots, N - 1$. Together with the condition of a fixed volume, $\Delta\Omega = 0$, this gives a system of N equations for determining all the Δr_n and λ

$$\begin{aligned} (2r_1 + r_2 + \Delta r_1 + \Delta r_2)h_{3/2}\Delta r_1 + \sum_{n=2}^{N-1} [(r_{n-1} + 2r_n + \Delta r_n)h_{n-1/2} + \\ + (2r_n + r_{n+1} + \Delta r_n + \Delta r_{n+1})h_{n+1/2}]\Delta r_n &= 0 \\ Kr_1 - B_{1/2}^- + \lambda(2r_1 + r_1 + 2\Delta r_1 + \Delta r_1)h_{1/2} + (K - C_{1/2}^-)\Delta r_1 - D_{1/2}\Delta r_1 &= 0 \\ B_{1/2}^+ - B_{1/2}^- + \lambda[(r_1 + 2r_1 + \Delta r_1 + 2\Delta r_1)h_{1/2} + (2r_1 + r_1 + 2\Delta r_1 + \Delta r_1)h_{1/2}] - \\ - D_{1/2}\Delta r_1 + (C_{1/2}^+ - C_{1/2}^-)\Delta r_1 - D_{1/2}\Delta r_1 &= 0 \\ B_{n-1/2}^+ - B_{n+1/2}^- + \lambda[(r_{n-1} + 2r_n + \Delta r_{n-1} + 2\Delta r_n)h_{n-1/2} + (2r_n + r_{n+1} + 2\Delta r_n + \\ + \Delta r_{n+1})h_{n+1/2}] - D_{n-1/2}\Delta r_{n-1} + (C_{n-1/2}^+ - C_{n+1/2}^-)\Delta r_n - D_{n+1/2}\Delta r_{n+1} &= 0 \\ n = 1, \dots, N - 1 \\ B^\pm = Arr' + rp \pm pr' \frac{h}{2}, \quad C^\pm = Ar' + p \pm \frac{2A}{h} r, \quad D = \frac{2A}{h} r, \quad \Delta r_N = 0 \end{aligned} \tag{2.5}$$

These equations enable us to determine all the increments Δr_n and the Lagrange multiplier λ and to carry out the next correction of the contour of the forebody. Quantities of the order of $h\Delta r$ occur in the coefficients of Δr_n in the first equation and in all the coefficients of λ together with the principal terms of order h . Apart from these, system (2.5) is linear, with a matrix of coefficients, only the first row of which differs from a four-diagonal matrix. In Newton’s problem with a fixed aspect ratio l with a free volume, the first equation drops out of system (2.5) while in the remaining ones $\lambda = 0$. The system of $N - 1$ equations thereby obtained is linear with a three-diagonal matrix of the coefficients,

which facilitates the construction of the optimum nose shape by the same method (see Ref. 32). Its volume $\Omega^0 = \Omega^0(l, M_\infty, \kappa)$.

At the beginning of the correction process, the initial contour is chosen in such a way that for fixed l and a volume $\Omega > \Omega^0$ the nose shape satisfies constraints (2.1). The contours obtained after the next correction satisfy the same constraints. A direct calculation of the flow around any such forebody gives the wave drag coefficient of the front face c_{x0} , the integral of the pressure forces χ and the flow parameters on the segment r^*f , and consequently the free terms and linear parts of the coefficients of system (2.5). An iteration procedure for solving it determines all the increments Δr_n . If in the expression for $\Delta\Omega$ (the penultimate relation of (2.4)) and in the first equation of system (2.5) we drop the quadratic terms, we obtain a linear system, the solution of which does not require iterations. In this case, however, the need arises to refine the volume of the corrected forebody.

Each cycle of correction includes a “single-parameter descent”, which consists of the following. In addition to the direct calculation of the flow around of the initial forebody, the flow around two corrected forebodies is also calculated. The radii of their front faces and the gently sloping parts are replaced by $r_n + s\Delta r_n$ with Δr_n obtained by the method described, and two values of the parameter s , for example 0.5 and 1. In the s, χ plane a parabola is drawn through the three points corresponding to this s and the initial nose shape ($s=0$): $\chi(s) = \chi(0) + a_1s + a_2s^2$; then the value of $s_m = -a_1/(2a_2)$ which gives a minimum of χ is determined, and from this the radii $r_n + s_m\Delta r_n$ of the new nose shape are found. This nose shape serves as the initial one for the next cycle. With each correction, the increments Δr_n are reduced, while the Lagrange multiplier λ approaches a constant value.

During the calculations the problem was found to be ill-posed, which manifests itself in a large spread in the eigenvalues of the matrix of the coefficients of Δr_n (the Hesse matrix) of the $N - 1$ equations (without the first) of system (2.5). The maximum and minimum eigenvalues may differ in value by several orders of magnitude. Hence, in the last cycles of the optimization procedure, an additional descent in directions was carried out, which gives eigenvectors corresponding to the least eigenvalues.

As Ω increases, situations are inevitable for which, for $n = k_1, \dots, N - 1$, the upper constraint on r from conditions (2.1) breaks down, i.e. when $r_{ki} < R$ the sum $r_{ki} + \Delta r_{ki} > R$. This means that for the chosen volume, the optimum contour of the forebody contains a cylindrical part. In such situations, the Δr_{ki} obtained must be replaced by $\Delta r_{ki} = R - r_{ki}$, and the remaining Δr_n are found from system (2.5) without the equations with the numbers indicated.

3. Calculation results

When calculating the flow around the forebody we distinguished two regions. The common boundary of the regions lay in the section $x = 2r_l$. In the neighbourhood of the front face, a computation grid was constructed, as shown in Fig. 3a, and the solution of Euler equations was obtained by the time relocation method using a Godunov scheme of the higher order and the algorithm used earlier in Refs 8,13. In this region, 207 nodes were placed on the body surface. Fig. 3b demonstrates the possibilities of the algorithm, in which, for $M_\infty = 4$ in steps of $\Delta M = 0.05$ we have drawn isomachs between the initial part of the forebody and the detached shock wave. In the second region (for $2r_l < x \leq L$), we calculated the x -supersonic flow in a cylindrical system of coordinates by the marching method using the MacCormack scheme with the algorithm given in Ref. 33. The number of grid nodes from the surface of the forebody to the shock was 84. In both regions, the shock fitting method was used.

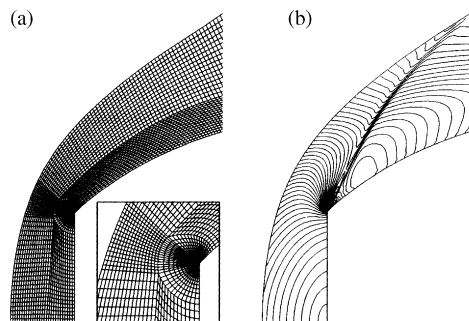


Fig. 3.

Depending on the aspect ratio and the volume of the forebody the number of points N in the segment t^+f of the sought contour varied from 60 to 275. In the region close to the front face the coordinates x_n were specified by the formula

$$x_n = 2r_1(k_1^{n-1} - 1)/(k_1^{25} - 1), \quad n = 1, \dots, 26; \quad k_1 = 1.1$$

by virtue of which the differences $x_{n+1} - x_n = h_{n+1/2}$ increase with distance from the face, while for $27 \leq n \leq N$

$$x_n = x_{26} + (x_N - x_{26})(k_2^{n-26} - 1)/(k_2^{N-26} - 1), \quad n = 27, \dots, N; \quad k_2 = 1.015$$

The direct method of optimization showed a high convergence rate: for a specified aspect ratio and volume when constructing the optimum nose shape it was necessary to calculate the flow around from 25 to 50 configurations.

The relative dimensions of the faces $\eta = r_1/R$ and the wave drag coefficients (C_x) of the nose shapes, constructed using the above method, for $\kappa = 1.4$, $M_\infty = 2$ and $M_\infty = 4$, various volume coefficients $C_\Omega^0 \leq C_\Omega \leq 1$ and two aspect ratios $l = 4$ and $l = 8$, are assembled in Table 1 under the numbers No. = 0, 1, ..., 6. For fixed M_∞ and l , the rows with No. = 0 correspond to Newton’s problem (with a free volume) solved using Euler equations. In this case, $C_\Omega = C_\Omega^0$, and the coefficients $C_x = C_x^0$ are a minimum. The quantities η^{MC} and C_x^{MC} , obtained in the same approximation when solving Newton’s problem previously in Ref. 8 using a control contour and the method of characteristics, are shown in the rows denoted in the side column by MC. The wave drag coefficients obtained for Newton’s problem in the present paper and in Ref. 8 are distinguished by a maximum on the unit of the last significant figure. Since the method used in Ref. 8 is only suitable for solving a narrow class of problems, the practical coincidence of C_x and C_x^{MC} is an additional confirmation of the effectiveness of the direct method of optimization employed. The difference between η and η^{MC} may reach 10–14%, which not only has no effect on the value of C_x , but also, for extremely small dimensions of the faces, is unimportant for applications.

In the rows of the table marked as NF (Newton’s formula), we show values of C_Ω and the dimensions of the faces η^N of the nose shapes constructed for Newton’s problem using Newton’s formula, and their wave-drag coefficients C_x^N - determined by integration of Euler equations. For these nose shapes, C_Ω is less than C_Ω^0 , when $M_\infty = 2$, by 10–11%, while for $M_\infty = 4$ it is less by 5–6%. A consequence of this is the large value of $\Delta C_x = (C_x^N/C_x - 1) \times 100$. When calculating it, the value of C_x was taken from the row with No. = 0. In the rows with No. = 1, 2, ..., 6, the values of

Table 1

Method of construction or no.	l	$C_\Omega \times 10^2$	$\eta^N \times 10^2$	$M_\infty = 2$			$M_\infty = 4$		
				$\eta \times 10^2$	$C_x \times 10^2$	ΔC_x	$\eta \times 10^2$	$C_x \times 10^2$	ΔC_x
NF		40.86	2.26			6.0			2.4
0	4	45.36 ($M_\infty = 2$)	3.54	9.76	6.81	3.2			
		42.95 ($M_\infty = 4$)	2.85				6.70	5.59	1.6
1		52	5.55	15.5	7.22	8.4	10.9	6.48	3.4
2		60	8.37	20.8	8.77	13.6	14.3	8.33	3.7
3		72	16.4	28.3	12.90	15.0	21.5	12.98	3.3
4		80	26.0	37.9	16.98	14.5	30.1	18.09	2.6
5		93	54.8	56.7	30.54	3.6	54.1	35.23	0.1
6		100	100	100	75.18	0.0	100	82.76	-0.1
MC				10.9	6.80		7.10	5.58	
NF		40.18	0.26			6.1			1.6
0	8	45.06 ($M_\infty = 2$)	0.54	2.10	2.22	0.9			
		42.67 ($M_\infty = 4$)	0.43				1.56	1.81	0.6
1		60	1.47	7.3	3.28	7.6	3.77	2.92	2.7
2		70	3.19	10.8	5.15	9.3	5.67	4.66	2.6
3		80	8.37	19.7	8.76	13.7	12.1	8.41	2.7
4		90	26.0	37.7	16.99	14.8	31.2	18.05	3.0
5		95	46.1	52.5	25.85	8.2	48.1	29.54	0.5
6		100	100	100	75.18	0.0	100	82.76	-0.1
MC				2.42	2.23		1.57	1.82	

ΔC_x were determined from the C_x^N of the nose shape with the same values of C_Ω as C_x . It is interesting to note that for fixed M_∞ and l the values of ΔC_x in the rows with No. = 0 are considerably less than in the rows marked as NF: by a factor of 1.5–2 for $l=4$ and a factor of 2.5–7 for $l=8$. Hence, for known $C_\Omega = C_\Omega^0$ Newton’s formula gives a nose shape which, within the framework of Euler equations, is closer to the optimum value than is obtained using the same formula in Newton’s problem.

For Newton’s problem the values of η^N are several times less than the dimensions of the faces of the nose shapes that are optimum in the Euler equations approximation. As C_Ω increases, this difference decreases and, naturally, disappears when $C_\Omega = 1$, when, irrespective of the model, the “optimum” nose shape is a blunt cylinder. The coefficients C_x^N were calculated by integration of the non-stationary Euler equations using the same algorithm that was used to calculate mixed flow in the “first” region (for $x \leq 2r$) of the direct method. The difference was the fact that the repeated calculation was carried out on a grid obtained by dividing the sides of the cells of the initial grid in half, while the coefficients C_x^N were found by linear extrapolation of the results of two calculations on the zero dimensions of the cell. A consideration of the calculation errors gives $\Delta C_x = -0.1\%$ for a cylinder ($C_\Omega = 1$) at $M_\infty = 4$.

Graphs of the relative dimensions of the front faces $\eta = r_1/R$ and of the cylindrical parts $\Delta = 1 - x_d/L$ against C_Ω for the values of M_∞ and l considered, obtained for the optimum nose shapes constructed, are shown in Fig. 4. The different markers correspond to the values of the aspect ratios and free-stream Mach numbers indicated in the left upper corner. The optimum nose shapes are shown in Fig. 5 and numbered in accordance with the side column of the table. The dashed curves were constructed for $M_\infty = 2$, while the continuous curves (including the segments of the ordinate axis and the upper horizontal) are for $M_\infty = 4$. For the aspect ratios considered, according to the hypersonic stabilization rule and the results obtained earlier in Ref. 8, the optimum contours, shown by the continuous curves, hardly change when $M_\infty > 4$.

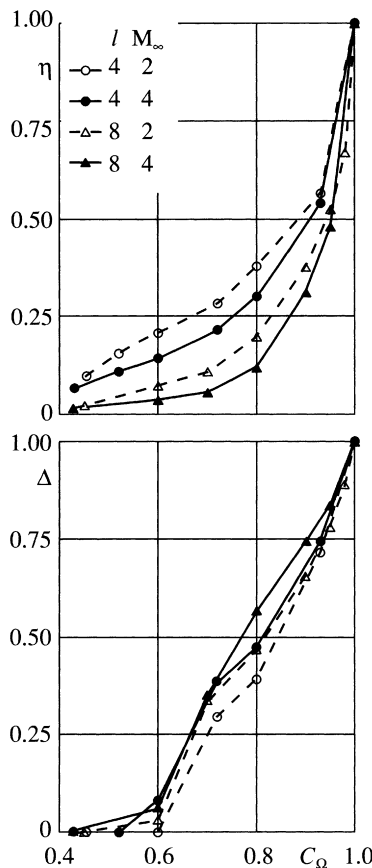


Fig. 4.

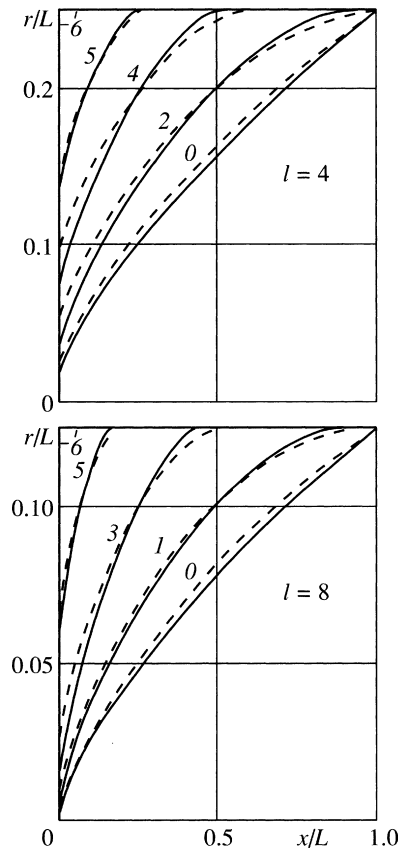


Fig. 5.

4. Conclusion

The limited nature of the range of applicability of the direct method described (contours and surfaces in a supersonic flow of perfect gas) does not exclude the presence of subsonic flow regions at the parts of the optimized configuration, like the region upstream the front face in the problem solved above, or base regions where gas is practically at rest. The latter are formed downstream the base faces that may occur when constructing complete body of fixed volume and external dimensions⁵ or divergent part of a nozzle,⁴ rather than constructing nose shapes. Together with purely supersonic configurations (including three-dimensional ones) this opens up fairly wide prospects for the use of this direct method.

Acknowledgements

This research was supported financially by the Russian Foundation for Basic Research (05-01-00846) and was performed within the framework of the Programme for the Support of the Leading Scientific Schools (NSh-9902.2006.1).

References

1. Newton I. *Mathematical Principles of Natural Philosophy*. Berkeley California: Univ. California Press; 1947.
2. Newton I. *Mathematical Principles of Natural Philosophy*. Moscow: Nauka; 1989.
3. Kraiko AN. The determination of bodies of minimum drag using the Newton and Busemann drag laws. *Prikl Mat Mekh* 1963;**27**(3):484–95.
4. Kraiko AN. *Variational Problems of Gas Dynamics*. Moscow: Nauka; 1979.
5. Kraiko AN, Pudovikov DYe, Yakunina GYe. *Theory of Close to Optimal Aerodynamic Shapes*. Moscow: Yanus-K; 2001.
6. Tikhomirov VM. *Accounts of Maxima and Minima*. Moscow: Nauka; 1986.
7. Lavrent'ev M, Lyusternik L. *Principles of the Variational Calculus. Vol. 1. Pt II*. Moscow and Leningrad: ONTI NKTP; 1935.

8. Kraiko AN, Pudovikov DYe, P'yankov KS, Tillyayeva NI. Axisymmetric nose shapes of specified aspect ratio, optimum or close to optimum with respect to wave drag. *Prikl Mat Mekh* 2003;**67**(5):795–828.
9. Eggers Jr AJ, Resnikoff MM, Dennis DH. Bodies of revolution having minimum drag at high supersonic speeds. *Rep NACA* 1957;(1306):12.
10. Eggers AJ. Nonslender bodies of revolution having minimum pressure drag. In: Miele A, editor. *Theory of Optimum Aerodynamic Shapes*. N.Y., L.: Acad. Press; 1965.
11. Kraiko AN. A nose shape of specified volume, optimum with respect to wave drag in the Newton's drag law approximation. *Prikl Mat Mekh* 1991;**55**(3):382–8.
12. Miele A. Slender bodies of minimum wave drag. In: Miele AS, editor. *The Theory of Optimum Aerodynamic Shapes*. New York: Academic Press; 1965.
13. Yefremov NL, Kraiko AN, P'yankov KS. The axisymmetric nose shape of minimum wave drag for given size and volume. *Prikl Mat Mekh* 2005;**69**(5):723–41.
14. Adelman HM, Haftka RT. Sensitivity analysis of discrete structural systems. *AIAA Journal* 1986;**24**(5):823–32.
15. Baysal O, Eleshaky ME. Aerodynamic sensitivity analysis methods for the compressible Euler equations. *Trans ASME J Fluid Enging* 1991;**113**(4):681–8.
16. Korivi VM, Newman PA, Taylor AC. III. Aerodynamic optimization studies using a 3-D supersonic Euler code with efficient calculation of sensitivity derivatives. AIAA Paper. 1994. No 94–4270.
17. Burgreen GW, Baysal O. Three-dimensional aerodynamic shape optimization of supersonic delta wings. AIAA Paper. 1994. No 94–4271.
18. Burgreen GW, Baysal O. Three-dimensional aerodynamic shape optimization using discrete sensitivity analysis. *AIAA Journal* 1996;**34**(9):1761–70.
19. Sung C, Know JH. Accurate aerodynamic sensitivity analysis using adjoint equations. *AIAA Journal* 2000;**38**(2):243–50.
20. Cliff SE, Reuther JJ, Saunders DA, Hicks RM. Single-point and multipoint aerodynamic shape optimization of high-speed civil transport. *J Aircraft* 2001;**38**(6):997–1005.
21. Taylor III AC, Green LL, Newman PA, Putko MM. Some advanced concepts in discrete aerodynamic sensitivity analysis. *AIAA Journal* 2003;**41**(7):1224–99.
22. Oyama A, Obayashi S, Nakahashi K, Nakamura T. Euler/Navier-Stokes optimization of supersonic wings based on multi-objective genetic algorithms. *AIAA Journal* 1999;**37**(10):1327–8.
23. Benini E, Tofollo A. Development of high-performance airfoils for axial flow compressors using evolutionary computation. *J Propuls and Pow* 2002;**18**(3):544–54.
24. Sasaki D, Obayashi S, Nakahashi K. Navier-Stokes optimization of supersonic wings with four objectives using evolutionary algorithm. *J Aircraft* 2002;**39**(4):621–9.
25. Chernyi GG. Supersonic flow around an airfoil close to a wedge shape. Trudy TsIAM im PI Baranova 1950; No 197. Also in *Gas Dynamics, Selected Works*. Vol 1, Edited by Kraiko AN. Moscow: Fizmatlit; 2000. p. 443–462.
26. Takovitskii SA. Convergence in the problem of optimising a wing of complex shape. *Zh Vychisl Mat Mat Fiz* 2002;**42**(5):690–7.
27. Takovitskii SA. Numerical optimization of the wing of a supersonic airplane. In: *Proc. 23rd Intern. Congr. Aeronaut. Sci. (ICAS)*. 2002. p. 232.1–7.
28. Takovitskii SA. Optimization of the wing of a supersonic aircraft. *Tekh Vozdush Flota* 2003;**1**:20–3.
29. Takovitskii SA. Pointed two-parameter power-law nose shapes of minimum wave drag. *Prikl Mat Mekh* 2003;**67**(5):829–35.
30. Takovitskii SA. An analytical solution in the problem of constructing an airfoil of minimum wave drag. *Izv Ross Akad Nauk MZhG* 2003;**6**:122–31.
31. Takovitskii SA. An analytical solution in the problem of constructing axisymmetric nose shapes of minimum wave drag. *Izv Ross Akad Nauk MZhG* 2006;**2**:155–62.
32. Takovitskii SA. The construction of axisymmetric nose shapes of minimum wave drag. *Prikl Mat Mekh* 2006;**70**(3):412–6.
33. Takovitskii SA. A method of calculating the supersonic flow around aircraft using multizone computation grids. *Trudy TsAGI* 1997;**2590**:24–32.

Translated by R.C.G.